

# Variations in the requirement for v-SNAREs in GLUT4 trafficking in adipocytes

Ping Zhao<sup>1,2,\*</sup>, Lu Yang<sup>1,3,\*</sup>, Jamie A. Lopez<sup>2</sup>, Junmei Fan<sup>1</sup>, James G. Burchfield<sup>2</sup>, Li Bai<sup>1</sup>, Wanjin Hong<sup>4</sup>, Tao Xu<sup>1,‡</sup> and David E. James<sup>2,‡</sup>

<sup>1</sup>National Laboratory of Biomacromolecules, Institute of Biophysics, Chinese Academy of Sciences, Beijing 100101, China

<sup>2</sup>Diabetes and Obesity Program, Garvan Institute of Medical Research, Sydney 2010, Australia

<sup>3</sup>Graduate University of the Chinese Academy of Sciences, Beijing 100039, China

<sup>4</sup>Institute of Molecular and Cell Biology, Singapore 138673, Singapore

\*These authors contributed equally to this work

‡Authors for correspondence (xutao@ibp.ac.cn; d.james@garvan.org.au)

Accepted 19 July 2009

Journal of Cell Science 122, 3472-3480 Published by The Company of Biologists 2009

doi:10.1242/jcs.047449

## Summary

Vesicle transport in eukaryotic cells is regulated by SNARE proteins, which play an intimate role in regulating the specificity of vesicle fusion between discrete intracellular organelles. In the present study we investigated the function and plasticity of v-SNAREs in insulin-regulated GLUT4 trafficking in adipocytes. Using a combination of knockout mice, v-SNARE cleavage by clostridial toxins and total internal reflection fluorescence microscopy, we interrogated the function of VAMPs 2, 3 and 8 in this process. Our studies reveal that the simultaneous disruption of VAMPs 2, 3 and 8 completely inhibited insulin-stimulated GLUT4 insertion into the plasma membrane, due to a block in vesicle docking at the plasma

membrane. These defects could be rescued by re-expression of VAMP2, VAMP3 or VAMP8 alone, but not VAMP7. These data indicate a plasticity in the requirement for v-SNAREs in GLUT4 trafficking to the plasma membrane and further define an important role for the v-SNARE proteins in pre-fusion docking of vesicles.

Supplementary material available online at

<http://jcs.biologists.org/cgi/content/full/122/19/3472/DC1>

Key words: SNARE proteins, Membrane transport, Vesicle docking, VAMP

## Introduction

The specificity of vesicle transport in eukaryotic cells is governed in large part by a high affinity interaction that occurs between membrane SNARE (soluble *N*-ethylmaleimide-sensitive factor attachment protein receptor) proteins found in the relevant donor and acceptor membranes. The formation of a SNARE complex involving SNARE proteins on the vesicle (v-SNAREs) and SNAREs on the target membrane (t-SNAREs) is central to membrane fusion, and is thought to provide the free energy required to promote fusion of lipid bilayers (Malsam et al., 2008). SNAREs play an important role in the delivery of membrane proteins to the plasma membrane (PM) (Pocard et al., 2007). Several different putative delivery pathways have been described, including rapid and slow recycling pathways as well as regulated delivery pathways as typified by the facilitative glucose transporter type 4 (GLUT4), which constitutes a key process for blood glucose control (Larance et al., 2008). This process is regulated by insulin, which triggers a signal transduction pathway involving the Ser/Thr kinase Akt. This releases an intracellular store of GLUT4 storage vesicles (GSVs), which dock and fuse with the PM (Ng et al., 2008). A SNARE complex comprising vesicle-associated membrane protein (VAMP2), synaptosomal-associated protein (SNAP23) and syntaxin-4 has been implicated in this process (Kawanishi et al., 2000). VAMP2 is found in GSVs, and SNAP23 and syntaxin-4 are found on the adipocyte PM. However, multiple v-SNAREs have been identified in GSVs including VAMPs 2, 3 and 8 (Larance et al., 2005). Moreover, these v-SNAREs have all been found to participate in exocytosis in other cell types (Bajno et al., 2000; Cosen-Binker et al., 2008; Schoch et al., 2001) and to form

complexes with syntaxin-4 and SNAP23 (Polgar et al., 2002). Furthermore, the role of VAMP2 in GLUT4 trafficking is controversial because some studies have shown that tetanus neurotoxin (TeNT), which proteolytically cleaves VAMP2, inhibits insulin-stimulated GLUT4 trafficking and glucose uptake (Randhawa et al., 2000), whereas others have found that this is not the case (Hajduch et al., 1997). Thus, it remains to be clarified which VAMPs are involved in GLUT4 trafficking in intact cells.

Whereas the assembly of SNARE complexes is thought to play a key role in membrane fusion, the involvement of SNAREs in pre-fusion steps such as membrane attachment (or 'docking') is controversial. In liposome fusion assays, the frequency of collisions between liposomes is so high that docking is not rate-limiting, thus precluding a formal analysis of the docking step using this method. On the one hand, a large number of interference studies in synapses and chromaffin cells have concluded that SNAREs, particularly v-SNAREs, are dispensable for docking (Borisovska et al., 2005; Hunt et al., 1994; Schoch et al., 2001). On the other hand, several observations in vitro provide indirect evidence that SNAREs (preferentially t-SNAREs) are required for docking before fusion (Schiavo et al., 1997; Vites et al., 2008). Unfortunately, most studies examining docking rely on morphological proximity to the PM based on electron microscopy (EM) images. However, it is not experimentally easy to capture short-lived intermediate stages such as docking. Moreover, the existence of redundant SNAREs during docking in biological systems could further complicate the analysis of experimental results.

Previously, we have defined the dynamic docking of GSVs employing high-resolution total internal reflection fluorescence

microscopy (TIRFM) in live adipocytes (Bai et al., 2007; Jiang et al., 2008). However, the molecular players underlying this docking stage remain elusive. In the current study, we have taken advantage of germline knockout mice combined with the expression of TeNT, to assess the role of different v-SNAREs in the trafficking of GLUT4 to the cell surface in response to insulin. Our data demonstrate that GSV trafficking to the PM can be functionally supported by different v-SNAREs or by VAMPs 2, 3 or 8. High-resolution TIRFM studies showed an essential role for v-SNAREs in the ‘docking’ of vesicles at the PM. Our data suggest that v-SNAREs do not exclusively define the specificity of membrane fusion reactions but, rather, that this appears to be dictated in part by the compartment that carries them.

## Results

**Absence of VAMP2 does not affect insulin-stimulated glucose uptake and GLUT4 externalization in MEF-derived adipocytes**  
VAMP2 has previously been implicated as a major v-SNARE regulating the docking and/or fusion of GSVs with the PM in adipocytes, in concert with the t-SNAREs SNAP23 and syntaxin-4. We set out to examine GLUT4 trafficking in adipocytes derived from VAMP2 knockout (ko) mice. The VAMP2 ko animals display neonatal lethality, and therefore we developed procedures for studying GLUT4 trafficking in adipocytes differentiated from mouse embryonic fibroblasts (MEFs) obtained from homozygous knockout embryos. As shown in Fig. 1, these cells were highly insulin-responsive in terms of insulin-regulated glucose transport and insulin-regulated GLUT4 translocation to the PM. Importantly, the loss of VAMP2 had no effect on the capacity of these MEF cells to differentiate into adipocytes in culture (supplementary material Fig. S1). Furthermore, lack of VAMP2 had no effect on the expression of syntaxin-4, SNAP23 and Munc18c, or other VAMP isoforms (Fig. 1A) and the localization of GLUT4 was indistinguishable from that seen in wild-type (wt) cells (supplementary material Fig. S4). We first investigated GLUT4 fusion using MEF-derived adipocytes retrovirally infected with the hemagglutinin (HA)-GLUT4 reporter. Treatment of VAMP2 wt and VAMP2 ko cells with 100 nM insulin for 20 minutes resulted in similar levels of HA-GLUT4 on the cell surface (Fig. 1B). The amount of HA-GLUT4 on the surface of the adipocytes was quantified and we observed no significant difference in labeling between wt and ko cells under both basal and insulin-treated conditions (Fig. 1C). Next, we examined insulin-induced glucose uptake in wt and VAMP2 ko adipocytes. Treatment of wt adipocytes with 1 and 100 nM insulin resulted in a ~3.5 and ~5.9-fold increase in glucose uptake, respectively (Fig. 1D). Interestingly, there was no significant defect in either basal or insulin-induced glucose uptake in the VAMP2 ko adipocytes as compared with wt controls. This demonstrates that endogenous GLUT4 trafficking is unaffected by loss of VAMP2.

We also used TIRFM to specifically examine the trafficking of enhanced green fluorescent protein (eGFP)-tagged GLUT4 in MEF-derived adipocytes. Our previous studies demonstrated that eGFP-tagged GLUT4 can be used to visualize single GSVs under TIRFM in 3T3-L1 adipocytes (Bai et al., 2007). As shown in Fig. 1E, insulin caused a time-dependent increase in GLUT4-eGFP fluorescence in the evanescent field. This is consistent with the time course for insulin-stimulated GLUT4 translocation to the PM in 3T3-L1 adipocytes. In agreement with the GLUT4 fusion data described above (Fig. 1B,C), we found that the absence of VAMP2 had no significant effect on the kinetics (Fig. 1F) or magnitude (Fig. 1G) of the insulin-dependent GLUT4 trafficking response.

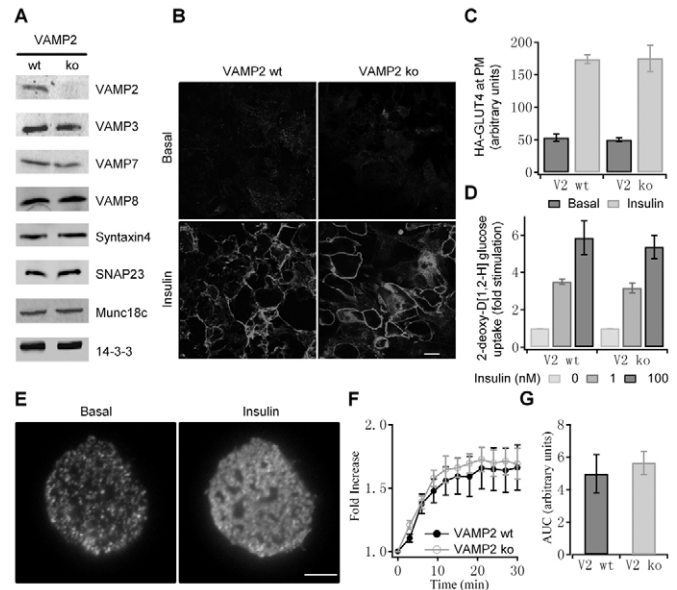


**Fig. 1.** Insulin-stimulated GLUT4 trafficking and glucose uptake in VAMP2 ko adipocytes. (A) Immunoblot analysis of VAMP2 ko MEF protein lysates. Lysates prepared from MEF-derived adipocytes of VAMP2 wt and ko mice were subjected to immunoblot analysis with antibodies specific for the indicated proteins. 14-3-3 was used as a loading control. (B) MEF cells were isolated from either VAMP2 (V2) wt or ko mice. Cells were infected with pBabe-HA-GLUT4 retrovirus and stained with HA antibody and Cy3-conjugated secondary antibody in order to detect externalized GLUT4 by confocal microscopy. Scale bar: 40  $\mu$ m. (C) HA-GLUT4 surface labeling in experiments similar to that shown in B was measured in VAMP2 wt or ko adipocytes under basal and insulin-treated conditions. Data represent mean  $\pm$  s.e.m. of values from four separate experiments, with between 238 and 311 cells being examined in each experiment. (D) Insulin-stimulated glucose transport in VAMP2 ko adipocytes. Uptake of 2-deoxy-D-[1, 2- $^3$ H] glucose was assayed in VAMP2 wt or ko adipocytes stimulated with the indicated concentration of insulin. Data represent mean  $\pm$  s.e.m. of three independent experiments and are expressed as fold stimulation of glucose uptake relative to that without insulin. (E) MEF cells were isolated from either VAMP2 wt or ko mice and differentiated into adipocytes in vitro. Adipocytes were electroporated with a GLUT4-eGFP plasmid and subjected to analysis by TIRFM two days later. TIRFM images in MEF-derived adipocytes incubated in the absence (Basal) or presence of insulin for 30 minutes. Scale bar: 10  $\mu$ m. (F) Time course of the change in fluorescence induced by insulin within the evanescent field in VAMP2 wt ( $n=10$  cells) and ko ( $n=15$  cells) adipocytes. Fluorescence was normalized to the value prior to insulin application. (G) Mean  $\pm$  s.e.m. of arbitrary units of the change in fluorescence from F. Data represent the fold increase in fluorescence induced by insulin from 0 to 30 minutes.

### VAMP2 and VAMP3 are dispensable for insulin-stimulated GLUT4 externalization in 3T3-L1 adipocytes

Given VAMP2 is considered to be the major v-SNARE mediating GLUT4 exocytosis (Williams and Pessin, 2008), the absence of a phenotype in cells lacking VAMP2 was surprising. The results suggested that VAMP2 is either unnecessary for insulin-stimulated GLUT4 trafficking, or that the cells that survived in culture had compensated for the complete lack of VAMP2, and thus did not reflect the importance of VAMP2 in GLUT4 trafficking. To test this hypothesis, we examined the effect of acute TeNT-induced cleavage of VAMP2 on insulin-stimulated GLUT4 trafficking in both 3T3-L1 adipocytes and MEF-derived adipocytes. TeNT has been shown to inactivate VAMP2 and VAMP3 by cleaving the peptide bond between amino acids Gln76Phe77 and Gln63Phe64, respectively, and has previously been shown to inhibit GLUT4 trafficking to the PM in L6 myotubes (Randhawa et al., 2000).

We constructed a GLUT4-eGFP-IRES-TeNT plasmid, allowing simultaneous expression of the toxin and a GLUT4 reporter. Expression of GLUT4-eGFP-IRES-TeNT effectively cleaved coexpressed VAMP2-eGFP and VAMP3-eGFP in either HEK 293T cells or 3T3-L1 adipocytes (Fig. 2B; supplementary material Fig. S3B). As shown in Fig. 2A, insulin caused a time-dependent increase in GLUT4-eGFP fluorescence in the evanescent field in differentiated 3T3-L1 adipocytes by TIRFM. Interestingly, transient transfection of the GLUT4-eGFP-IRES-TeNT plasmid had no significant effect on either the kinetics (Fig. 2C) or the magnitude (Fig. 2D) of insulin-induced GLUT4 translocation in differentiated 3T3-L1 adipocytes by TIRFM. We also investigated GLUT4 fusion using 3T3-L1 adipocytes transfected with the HA-GLUT4-GFP cDNA. To distinguish GFP-tagged GLUT4, we used a TeNT-IRES-mOrange construct, which can also effectively

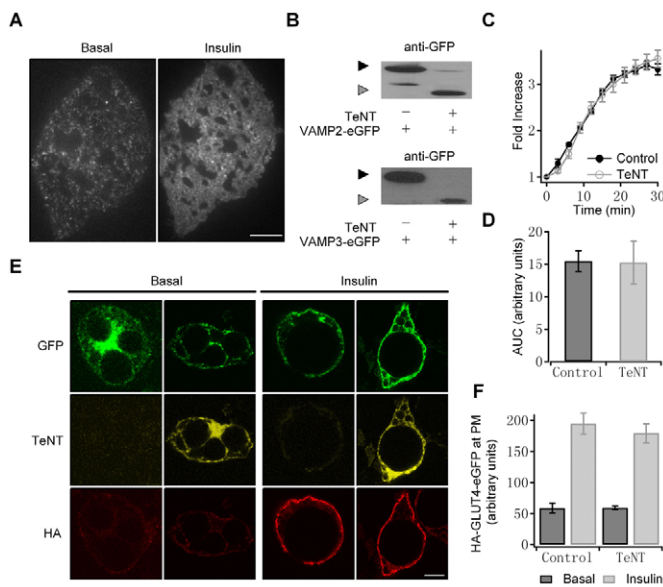


**Fig. 2.** Inactivation of VAMP2 and VAMP3 does not affect GLUT4 externalization in 3T3-L1 adipocytes. (A) 3T3-L1 adipocytes were transfected with GLUT4-eGFP and TIRFM images taken in 3T3-L1 adipocytes incubated in the absence (Basal) or presence of insulin for 30 minutes. Scale bar: 10  $\mu$ m. (B) Tetanus toxin light chain can effectively cleave VAMP2-eGFP or VAMP3-eGFP chimeras in HEK 293T cells. HEK 293T cells were transfected with VAMP2-eGFP (upper panel) and VAMP3-eGFP (lower panel) in the absence (-) or presence (+) of GLUT4-eGFP-IRES-TeNT cDNA as shown. Total cell lysates from all samples were separated by 10% SDS-PAGE and immunoblotted with anti-GFP antibodies. The black and gray arrowheads indicate the uncleaved and cleaved fragments of the v-SNAREs-eGFP, respectively. (C) Time course of the change in fluorescence induced by insulin within the evanescent field in control ( $n=11$  cells) and GLUT4-eGFP-IRES-TeNT-transfected ( $n=7$  cells) 3T3-L1 adipocytes. Fluorescence was normalized to the value prior to insulin application. (D) Mean  $\pm$  s.e.m. of area under the curve (arbitrary units) of the change in fluorescence from C. Data represent the fold increase in fluorescence induced by insulin from 0 to 30 minutes. (E) 3T3-L1 adipocytes were transfected with HA-GLUT4-GFP cDNA in the absence (left) or presence (right) of TeNT-IRES-mOrange cDNA and processed for indirect immunofluorescence using anti-HA antibodies under basal and insulin-treated conditions. GLUT4-GFP is shown in green (upper panel), TeNT-IRES-mOrange is shown in yellow (middle panel) and HA antibody labeling is shown in red (lower panel). Representative images are shown. Scale bar: 10  $\mu$ m. (F) Quantification of surface HA fluorescence measured from adipocytes in the absence or presence of TeNT-IRES-mOrange cDNA under both basal and insulin-treated conditions from E. Data represent mean  $\pm$  s.e.m. of values from three separate experiments, with 25-70 cells quantified per experiment.

cleave coexpressed VAMP2-eGFP and VAMP3-eGFP in 3T3-L1 adipocytes (supplementary material Fig. S3B). The insulin-induced fusion of GLUT4 with the PM was monitored in these cells by measurement of cell-surface labeling with antibodies to the HA tag (Shewan et al., 2003). Again, TeNT-IRES-mOrange did not significantly affect insulin-induced surface deployment of HA-GLUT4 (Fig. 2E,F).

#### VAMP2 and VAMP3 are dispensable for insulin-stimulated GLUT4 externalization in MEF-derived adipocytes

We expressed TeNT-IRES-mOrange together with GLUT4-eGFP in order to inactivate both VAMP2 and VAMP3 in MEF-derived adipocytes. Consistent with studies in 3T3-L1 adipocytes, coexpression of TeNT-IRES-mOrange and HA-GLUT4 had no significant effect on GSV fusion (Fig. 3A,B) under basal or insulin-treated conditions, and expression of GLUT4-eGFP-IRES-TeNT had no significant effect on the kinetics (Fig. 3C) or magnitude (Fig. 3D) of the insulin-induced GLUT4 translocation response. Thus, acute loss of VAMPs 2 and 3 does not effect insulin-stimulated GLUT4 trafficking, which argues against a compensatory response in the VAMP2 ko MEFs and supports the conclusion that VAMPs 2 and 3 are not required for insulin-stimulated GLUT4 PM insertion.

#### Disruption of VAMP2, VAMP3 and VAMP8 inhibits insulin-stimulated GLUT4 externalization in adipocytes

VAMP8 has recently been shown to be a crucial regulator of secretory events in the exocrine system (Wang et al., 2007), playing an important role in amylase secretion in salivary glands

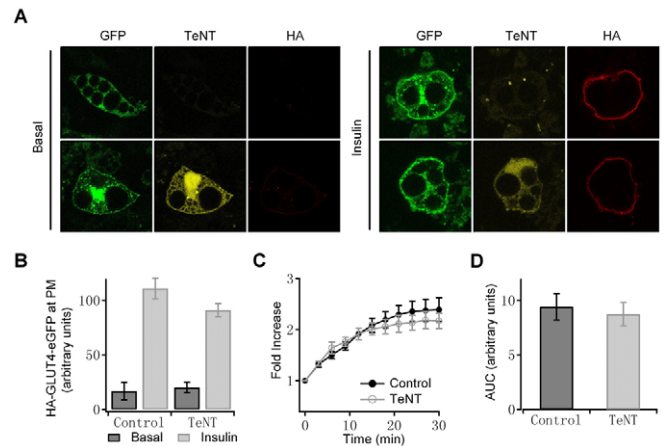


**Fig. 3.** Inactivation of VAMP2 and VAMP3 does not affect GLUT4 externalization in MEF adipocytes. (A) MEF-derived adipocytes were transfected with HA-GLUT4-GFP in the absence (upper panel) or presence (lower panel) of TeNT-IRES-mOrange cDNA and processed for indirect immunofluorescence of anti-HA antibodies under basal and insulin-treated conditions. GFP is shown in green (left), TeNT-IRES-mOrange is shown in yellow (middle) and HA antibody labeling is shown in red (right). Scale bar: 10  $\mu$ m. (B) HA-GLUT4 surface labeling was quantified in experiments similar to that shown in A. Measurements were taken from cells in the absence or presence of TeNT-IRES-mOrange cDNA under basal and insulin-treated conditions. Data represent mean  $\pm$  s.e.m. of values from three separate experiments, with between 39 and 46 cells being examined in each experiment. (C) Time course of the change in fluorescence induced by insulin within the evanescent field in control ( $n=10$  cells) and GLUT4-eGFP-IRES-TeNT-transfected ( $n=10$  cells) adipocytes derived from MEFs. (D) Mean  $\pm$  s.e.m. of arbitrary units of the change in fluorescence from C. Data represent the fold increase in fluorescence induced by insulin from 0 to 30 minutes.

and zymogen granule exocytosis in the pancreatic acinar cells. We have previously observed the presence of VAMP8 in GLUT4-containing membrane fractions (Larance et al., 2005). To determine whether VAMP8 plays a role in GLUT4 exocytosis, we studied differentiated MEF cells from VAMP8 wt or VAMP8 ko mice. The loss of VAMP8 had no effect on the capacity of these MEF cells to differentiate into adipocytes in culture (supplementary material Fig. S1). Furthermore, lack of VAMP8 had no effect on the expression of syntaxin-4, SNAP23 and Munc18c, or other VAMP isoforms (Fig. 4A). To determine the function of VAMP8, we investigated GLUT4 fusion using VAMP8 wt and ko MEF-derived adipocytes transfected with the HA-GLUT4-GFP cDNA. Treatment of VAMP8 wt and ko cells with 100 nM insulin for 30 minutes resulted in similar levels of HA-GLUT4 insertion in the cell surface (Fig. 4B). The amount of HA-GLUT4 fused with the PM of the adipocytes was quantified under basal and insulin-treated conditions (Fig. 4C), with no significant difference in labeling under any condition between VAMP8 wt and ko cells. By monitoring insulin-induced GLUT4-eGFP translocation to the PM under TIRFM, we found no significant difference between VAMP8 ko and wt MEF-derived adipocytes (Fig. 4D,E). These results suggest that either VAMP8 is not involved in this exocytic pathway or that other VAMP isoforms are compensating in the absence of VAMP8.

Emerging evidence suggests that intracellular membrane-fusion reactions are not dependent on specific v-SNARE molecules, with several studies now showing that v-SNARE function can be substituted by different v-SNARE isoforms (Borisovska et al., 2005; Liu and Barlowe, 2002). To address the issue of VAMP redundancy, we next investigated GLUT4 trafficking in the absence of all three VAMP isoforms known to be associated with GSVs (VAMPs 2, 3 and 8). This was achieved by the transient transfection of GLUT4-eGFP-IRES-TeNT in MEF-derived adipocytes from VAMP8 ko mice. Cleavage of VAMPs 2 and 3 on a VAMP8 ko background drastically inhibited insulin-stimulated GLUT4-eGFP externalization in the cell-surface as compared with VAMP8 wt adipocytes transfected with GLUT4-eGFP (Fig. 4F). The lack of functional VAMP2, VAMP3 and VAMP8 culminated in a significant ( $P < 0.001$ ) 86% reduction in insulin-dependent GLUT4 trafficking to the PM (Fig. 4G) compared with wt controls. Consistently, coexpression of TeNT-IRES-mOrange and HA-GLUT4-GFP in VAMP8 ko cells also blocked insertion of HA-GLUT4 into the PM (Fig. 4B), resulting in a significant ( $P < 0.001$ ) 79% decrease in basal labeling and 99% reduction in insulin-induced HA labeling compared with the VAMP8 wt controls (Fig. 4C).

#### Re-expression of VAMP2, VAMP3 or VAMP8 alone restores normal GLUT4 externalization

We next sought to clarify the function of the individual VAMP isoforms in this exocytic process. For these experiments, we cotransfected the GLUT4-eGFP-IRES-TeNT plasmid with TeNT-insensitive VAMP2-eGFP (TI-VAMP2-eGFP) or TeNT-insensitive VAMP3-eGFP (TI-VAMP3-eGFP) or VAMP8-eGFP into VAMP8 ko adipocytes. As expected, the TI-VAMP2-eGFP and TI-VAMP3-eGFP were significantly resistant to cleavage by TeNT, in contrast to wt VAMP2 and VAMP3 in HEK 293T cells and MEF-derived adipocytes (Fig. 5A; supplementary material Fig. S3A). Interestingly, cotransfection of GLUT4-eGFP-IRES-TeNT along with toxin-resistant mutants of VAMP2 (Fig. 5B,C), VAMP3 (Fig. 5D,E) or wt VAMP8 (Fig. 5F,G), each completely rescued the impairment in insulin-regulated GLUT4 trafficking to the PM. Co-

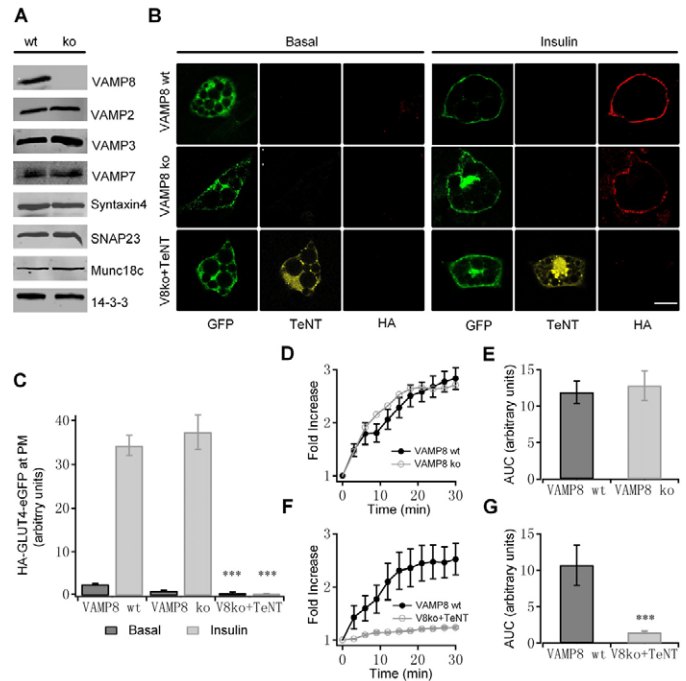


**Fig. 4.** Absence of VAMP2, VAMP3 and VAMP8 inhibited insulin-stimulated GLUT4 insertion into the PM in adipocytes. (A) Immunoblot analysis of VAMP8 ko MEF protein lysates. Lysates prepared from MEF-derived adipocytes of VAMP8 wt and ko mice were subjected to immunoblot analysis with antibodies specific for the indicated proteins. 14-3-3 was used as a loading control. (B) VAMP8 wt adipocytes were transfected with HA-GLUT4-GFP (upper panel), and VAMP8 ko adipocytes were transfected with HA-GLUT4-GFP in the absence (middle panel) or presence (lower panel) of TeNT-IRES-mOrange cDNA and processed for indirect immunofluorescence of anti-HA antibodies under basal and insulin-treated conditions. GFP is shown in green (left), TeNT-IRES-mOrange is shown in yellow (middle) and HA antibody labeling is shown in red (right). Scale bar: 10  $\mu$ m. (C) HA-GLUT4 surface labeling was quantified in experiments similar to that shown in B. Measurements were taken from VAMP8 wt adipocytes and from VAMP8 ko adipocytes in the absence or presence of TeNT-IRES-mOrange cDNA under basal and insulin-treated conditions. Data are mean  $\pm$  s.e.m. of values from three separate experiments, with between 34 and 38 cells being examined in each experiment. Asterisks (\*\*\*) indicate a statistically significant ( $P < 0.001$ ) difference in TeNT-treated VAMP8 ko cells compared with VAMP8 wt cells under basal and insulin-treated conditions. (D) Time course of the change in fluorescence induced by insulin within the evanescent field in adipocytes transfected with GLUT4-eGFP from VAMP8 wt ( $n=10$  cells) and VAMP8 ko ( $n=8$  cells) adipocytes. Fluorescence was normalized to the value prior to insulin application. (E) Mean  $\pm$  s.e.m. of arbitrary units of the change in fluorescence from adipocytes in D. Data represent the fold increase in fluorescence induced by insulin from 0 to 30 minutes. (F) VAMP8 wt or ko adipocytes were transfected with GLUT4-eGFP and GLUT4-eGFP-IRES-TeNT separately. The increase in evanescent-field fluorescence induced by insulin is blocked by transfection of GLUT4-eGFP-IRES-TeNT in VAMP8 ko mice. (G) Mean  $\pm$  s.e.m. of arbitrary units of the change in fluorescence from F. Data represent the fold increase in fluorescence induced by insulin from 0 to 30 minutes. Asterisks (\*\*\*) indicate a statistically significant ( $P < 0.001$ ) difference of the TeNT-treated VAMP8 ko ( $n=30$  cells) compared with VAMP8 wt ( $n=5$  cells) adipocytes.

transfection of GLUT4-eGFP-IRES-TeNT with wt VAMP7 (Fig. 5H,I) did not rescue the impairment in insulin-regulated GLUT4 trafficking to the PM. These data demonstrate that GLUT4 trafficking to the PM can be functionally supported by either of the VAMP isoforms 2, 3 or 8 but not VAMP7. These data suggest that there might be some degree of specificity that is shared between VAMPs 2, 3 and 8, but not VAMP7.

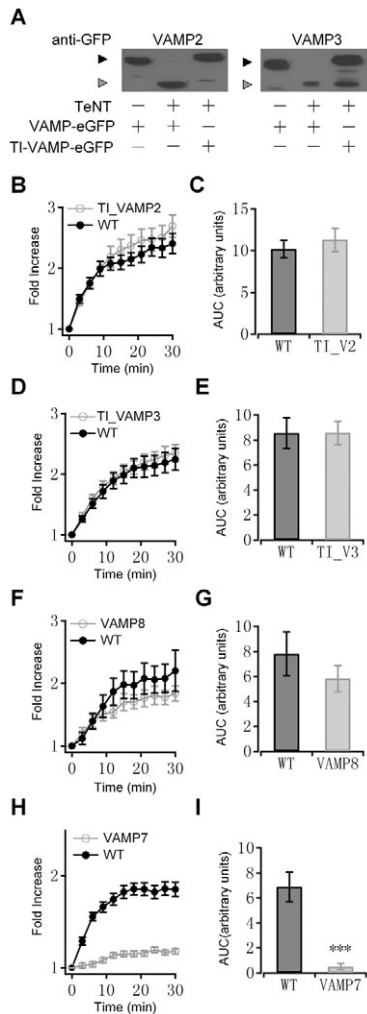


**Fig. 5.** Re-expression of VAMP2, VAMP3 or VAMP8 rescued insulin stimulated GLUT4 externalization in TeNT transfected VAMP8 ko adipocytes. (A) Tetanus toxin light chain can effectively cleave wild-type but not toxin insensitive VAMP2-eGFP or VAMP3-eGFP chimeras in HEK 293T cells. HEK 293T cells were transfected with wild-type VAMP2-eGFP or toxin insensitive VAMP2 (TI-VAMP2-eGFP) (left panel), wild-type VAMP3-eGFP or toxin insensitive VAMP3 (TI-VAMP3-eGFP) (right panel) in the absence (–) or presence (+) of GLUT4-eGFP-IRES-TeNT cDNA as shown. Total cell lysates from all samples were separated by 10% SDS-PAGE and immunoblotted with anti-GFP antibodies. The black and grey arrowheads indicate the uncleaved and cleaved fragments of VAMP2-eGFP or VAMP3-eGFP, respectively. (B,D,F,H) VAMP8 wt adipocytes were transfected with GLUT4-eGFP and VAMP8 ko adipocytes were transfected with GLUT4-eGFP-IRES-TeNT and TI-VAMP2 (B), TI-VAMP3 (D), VAMP8-IRES-mOrange (F) and VAMP7 (H). Insulin-induced evanescent-field fluorescence increase is rescued by restoration of VAMP expression using TI-VAMP2 ( $n=11$  cells), control ( $n=10$  cells); TI-VAMP3 ( $n=20$  cells), control ( $n=9$  cells); or VAMP8 ( $n=10$  cells), control ( $n=5$  cells) but not by over-expression of VAMP7 ( $n=30$  cells), control ( $n=25$  cells) in TeNT transfected VAMP8 ko adipocytes compared with VAMP8 wt adipocytes. (C,E,G,I) Mean  $\pm$  s.e.m. of arbitrary units of the change in fluorescence from (B,D,F,H). There are no statistically significant differences between TI-VAMP2, TI-VAMP3, or VAMP8 in TeNT transfected VAMP8 ko adipocytes compared with VAMP8 wt adipocytes, whereas it is significant different between over-expression of VAMP7 in TeNT transfected VAMP8 ko adipocytes compared with VAMP8 wt adipocytes ( $P<0.001$ ).

#### v-SNARE controls the docking of vesicles at the PM

We have previously described the docking of GSVs underneath the PM, which were characterized by vesicles that enter the evanescent field with a sharp angle, stay immobilized for at least 1 second, and

then disappeared suddenly, without spreading of the fluorescence that is characteristic of fusion (Bai et al., 2007). A representative docking event is depicted in the kymograph in Fig. 6A. Quantification of vesicles within the TIRF zone revealed that the lack of functional VAMP2, VAMP3 and VAMP8 had no significant effect on the movement of GSVs from cytoplasm into the TIRF zone, as determined by measuring the density of GSVs in the evanescent field in the absence or presence of insulin (Fig. 6B). By contrast, in the absence of VAMP2, VAMP3 and VAMP8, most GSVs from cytoplasm entered the TIRF zone transiently (less than one second) without a stabilized docking state (see lower panel of Fig. 6A). The rate of docking events was almost completely inhibited under both basal and insulin-treated conditions (Fig. 6C). Quantification of this effect revealed that loss of the three VAMPs significantly reduced the basal docking events by 92% ( $P<0.01$ ), and by 95% ( $P<0.001$ ) in the presence of insulin, as compared with wt controls. These data strongly argue that v-SNAREs are involved in the stabilized docking of GSVs at the PM.

#### Colocalization of v-SNAREs with GSVs

To further verify which VAMPs reside on GSVs and co-migrate with GLUT4 towards the PM, we co-transfected MEF-derived adipocytes with GLUT4 tagged with monomeric Kusabira Orange (GLUT4-mKO) in combination with eGFP-tagged v-SNAREs. Using a double-channel TIRFM system, we first identified docking GSVs based on their characteristic movement of GLUT4-mKO as previously described (Bai et al., 2007; Jiang et al., 2008). Then we verified that VAMP2, 3 or 8 can be found associated with docking GSVs, as represented by superimposed trajectories shown in Fig. 7A. Under basal conditions we estimated that ~38% of docking GSVs contained VAMP3, whereas ~61% and ~56% of GSVs contained VAMP2 and VAMP8, respectively (Fig. 7B). Insulin treatment had no significant effect on the percentage localization of VAMPs with docking GSVs.

We also sought to identify the proportion of v-SNAREs on purified intracellular GSVs. In these experiments, a low density microsomal fraction that is enriched in GSVs was isolated from 3T3-L1 adipocytes retrovirally infected with GLUT4-eGFP. These membrane fractions were bound to coverslips coated with poly-L-lysine and labeled with antibodies for VAMP2, VAMP3, VAMP8 or combinations of VAMPs 2 and 3 or VAMPs 2 and 8. Under basal conditions we found that ~39% of intracellular GSVs contained VAMP3, whereas ~27% and ~22% of intracellular GSVs contained VAMP2 and VAMP8, respectively (Fig. 7C,D). Interestingly, we found that there was a small population of GSVs containing both VAMP2 and VAMP3 (~16%) or VAMP2 and VAMP8 (~9%) (Fig. 7C,D). This colocalization was not affected dramatically by insulin treatment. Importantly, we observed a significant 73% colocalization between GLUT4 and the insulin responsive amino peptidase (IRAP) (supplementary material Fig. S2), as previously reported (Jiang et al., 2008).

#### Discussion

##### Functional redundancy of v-SNAREs in insulin-stimulated GLUT4 trafficking in adipocytes

In this study, we show that the presence of any one of the v-SNAREs VAMP2, VAMP3 or VAMP8, suffices for insulin-stimulated GLUT4 trafficking in the adipocyte and, in fact, using a knockout/rescue strategy we were unable to find any unique functional role for any one of these v-SNAREs in GLUT4 externalization. The observation that VAMP3 and VAMP8 can function in this pathway was

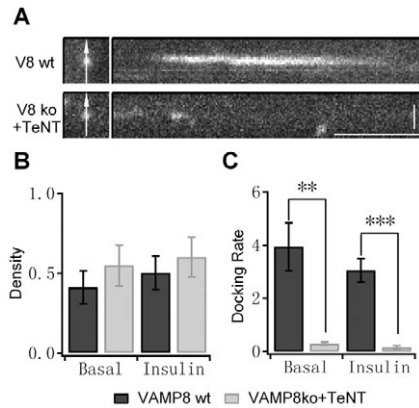


**Fig. 6.** Absence of VAMP2-, VAMP3- and VAMP8-blocked docking of GSVs. (A) Kymographs depicting individual GSV docking events. Each image depicts individual vesicle sections from the time-lapse sequences. These images are from a stack of 200 images at a frame rate of 5 Hz. The arrow indicates the direction in the kymograph. The vertical scale bar represents 1  $\mu\text{m}$  and the horizontal time bar represents 10 seconds. Kymographs depicting typical docking GSVs from VAMP8 wt adipocytes transfected with GLUT4-eGFP (upper panel) as compared with transient appearance of GSVs in the TIRF zone from VAMP8 ko cells transfected with GLUT4-eGFP-IRES-TeNT (lower panel). (B) Measurement of the vesicle density ( $\mu\text{m}^{-2}$ ) in the TIRF zone of MEF-derived adipocytes from VAMP8 wt cells transfected with GLUT4-eGFP ( $n=3$  cells) and VAMP8 ko cells transfected with GLUT4-eGFP-IRES-TeNT ( $n=6$  cells) in the absence or presence of insulin for 30 minutes. (C) The averaged docking rate (in  $10^{-3} \mu\text{m}^{-2}/\text{second}$ ) is dramatically decreased in VAMP8 ko adipocytes transfected with GLUT4-eGFP-IRES-TeNT compared with VAMP8 wt adipocytes transfected with GLUT4-eGFP in both the absence (\*\*  $P<0.01$ ) or presence of insulin (\*\*\*)  $P<0.001$ ).

unexpected, considering that only VAMP2 mediates this pathway in L6 myoblasts (Randhawa et al., 2000), but was consistent with a role for VAMPs 3 and 8 in exocytic trafficking to the PM. There is growing evidence to suggest that many SNARE-mediated trafficking steps utilize functionally redundant v-SNAREs proteins. In yeast for example, loss of the R-SNARE Sec22p, a protein that regulates ER-Golgi trafficking, can be functionally compensated through upregulation of the related R-SNARE Ykt6p (Liu and Barlowe, 2002). Furthermore, previous studies in chromaffin cells have shown that, in the absence of VAMP2,  $\text{Ca}^{2+}$ -triggered exocytosis measured by membrane capacitance is only partially inhibited. However, expression of TeNT in VAMP2 ko cells completely abolished secretion. Interestingly, reintroducing either of the VAMP isoforms VAMP2 or VAMP3 adequately rescued this secretion defect (Borisovska et al., 2005). Our experiments with the VAMP isoforms in the adipocyte extend these findings and highlight the importance of SNARE isoforms, not only in the differential regulation of individual vesicle trafficking events, but also in serving a compensatory function should a defect occur.

Although it has been proposed that VAMP2 and VAMP3 function in insulin-stimulated GLUT4 externalization via complexing with their cognate t-SNAREs syntaxin-4 and SNAP23 (Cheatham et al., 1996; Martin et al., 1998; Olson et al., 1997), it is unclear whether other VAMPs could act redundantly or substitute for VAMPs 2 and 3 in their absence. Hajduch et al. (Hajduch et al., 1997) has shown that complete loss of both VAMPs 2 and 3 via tetanus-toxin-mediated proteolysis produced no effect on the ability of insulin to stimulate glucose transport or GLUT4 trafficking to the PM in freshly isolated rat adipocytes. Another study also reported minimal

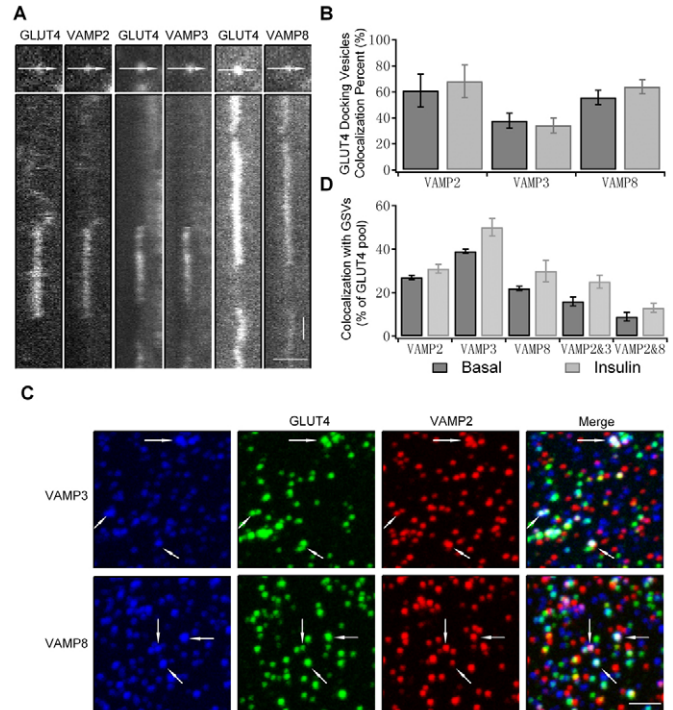


**Fig. 7.** Vesicle colocalization analysis between GLUT4 and VAMP 2, 3 and 8. (A) Kymographs depicting individual GSV docking events positive for VAMP2, 3 or 8 from 3T3-L1 adipocytes transfected with GLUT4-mKO and VAMP2-eGFP, VAMP3-eGFP or VAMP8-eGFP. Each image depicts individual vesicle sections from the time-lapse sequences. These images are from a stack of 300 images at a frame rate of 2.8 Hz. The arrow indicates the direction in the kymograph. The horizontal scale bar represents 1  $\mu\text{m}$  and the vertical time bar represents 10 seconds. (B) Percentage of colocalized docking events between GLUT4 and VAMP2-, 3- or 8-positive vesicles under basal and insulin-treated conditions. Data are normalized to the total amount of GLUT4 docking events from at least three cells. Approximately 90 docking events were analyzed per cell. (C) Intracellular vesicle colocalization analysis between GLUT4 and VAMPs 2, 3 and 8. LDM was isolated from 3T3-L1 adipocytes retrovirally infected with GLUT4-eGFP (green) and bound to coverslips coated with poly-L-lysine. VAMP2 was detected using a cy3-conjugated secondary antibody (red), and VAMP3 and VAMP8 were detected using cy5-conjugated secondary antibodies (blue). The arrows indicate the GLUT4-positive vesicles containing both VAMP2 and VAMP3 (upper panel) or VAMP2 and VAMP8 (lower panel). Scale bar: 2  $\mu\text{m}$ . (D) Percentage of colocalized GLUT4 and VAMPs 2, 3 or 8 from LDM-derived intracellular vesicles under basal and insulin-treated conditions. Data are normalized to the total amount of GLUT4-positive vesicles. Data represent mean  $\pm$  s.e.m. of values from three independent experiments.

(15%) inhibition of the insulin-dependent glucose uptake after treatment with Botulinum toxin type B (BoNT/B) in permeabilized 3T3-L1 cells, despite the fact that BoNT/B cleaved the majority of VAMPs 2 and 3 (Tamori et al., 1996). These studies are consistent with our results from 3T3-L1 adipocytes and mouse MEF-derived adipocytes. By contrast, BoNT/B has been shown to inhibit glucose uptake in 3T3-L1 adipocytes by 64% (Chen et al., 1997).

Recently, it has been shown that siRNA-mediated VAMP2 knockdown resulted in a 60% diminution of myc-GLUT4-GFP externalization in 3T3-L1 cells (Williams and Pessin et al., 2008). This discrepancy is surprising and the reason is unclear. One possibility is that the discrepancy might arise from the use of different cells and different intervention methods. Whereas RNAi might produce non-specific off-target effects, complete knockout of VAMP2 could suffer from developmental compensation in

adipocytes, which restores the insulin-stimulated GLUT4 trafficking to the PM.

However, this form of compensation does not explain our results from cells treated with tetanus toxin. Indeed, we were initially very surprised by this discrepancy and decided to confirm our result by different intervention methods combined with different functional assays for insulin-stimulated GLUT4 externalization. Regardless of the methods used, we observed no inhibition of insulin-stimulated GLUT4 externalization in either 3T3-L1 adipocytes or MEF-derived adipocytes. Apparently, further studies will be needed to clarify this discrepancy. A major question arising from these studies is whether one of the three v-SNAREs studied here is the true v-SNARE for GLUT4 trafficking under physiological conditions and its absence is simply compensated for by an indirect mechanism such as re-routing of GLUT4 via an alternate pathway. Such a hypothesis would imply that v-SNAREs are specifically sorted into discrete vesicle compartments in wild type cells. However, this does not appear to be the case. Using either TIRFM in intact cells or immunofluorescence labeling of membranes we observed considerable co-localization between each of the v-SNAREs VAMP2, 3 and 8 (Fig. 7) with GLUT4. Consistent with these observations, GSV populations containing both VAMP2 and 3 or VAMP2 and 8 are discernible in adipocytes. Furthermore, in the absence of VAMP2 the distribution of GLUT4 between endosomes and the 'GSV' pool is indistinguishable from wt cells (supplementary material Fig. S4), suggesting that loss of one or more VAMPs does not alter GLUT4 sorting.

On the basis of this observation, we speculate that VAMPs 2, 3 and 8 might operate as v-SNAREs for GSVs interchangeably, or even co-operatively on individual vesicles, and that there is no evidence a priori to support a model whereby these molecules define discrete vesicle transport pathways to the PM. This is intriguing in light of the fact that no major function other than SNARE complex formation has been described for these molecules. The t-SNAREs, however, have been shown to bind multiple effectors (Bao et al., 2008; Latham et al., 2006), which are likely to control their function in a regulated manner and provide specificity to SNARE complex assembly.

#### The functional role of v-SNAREs in insulin-stimulated GLUT4 trafficking

A major aim of this study was to address which step(s) in GSV exocytosis is(are) regulated by the v-SNARE. We have previously used high-frequency TIRFM to study the trafficking of eGFP-tagged GLUT4 in 3T3-L1 adipocytes (Bai et al., 2007; Li et al., 2004). Using this methodology and by analyzing the behavior of individual vesicles, we have dissected the final stages of GLUT4 exocytosis into several discrete steps, including translocation, docking and fusion. Our data together with that from others in the field have shown that these events are key targets for insulin action (Huang et al., 2007; Lizunov et al., 2005). In this study, the deletion of all functional VAMPs that are required for insulin-stimulated GLUT4 trafficking provided us the unique opportunity to determine which of the above mentioned steps are mediated by VAMPs. Importantly, the density of GSVs within the evanescent field was not significantly affected in the absence of functional v-SNAREs. This suggests that the translocation of vesicles from cytoplasm towards the PM is unperturbed. Our previous data suggest that some GSVs (mainly insulin-responsive GSVs) approach the PM rapidly from deep inside the cell at a perpendicular or steep angle, followed by a docking step at the PM that lasts several seconds. Most of these docked vesicles

move back to the cytosol without fusion under basal conditions, whereas insulin stimulation increases the percentage of fusion-competent docked vesicles. These data suggest the docked GSVs have a short dwell time and are in rapid dynamic exchange with the cytosolic pool, which makes the capture of docked GSVs by EM less favorable. The lack of accumulation of docked vesicles in adipocytes is in contrast with that in neurons and endocrine cells (Toonen et al., 2006; Voets et al., 2001). We found that these dynamic docking steps were completely absent in cells in which the expression of VAMPs 2, 3 and 8 were all ablated, suggesting an indispensable role for VAMPs in the docking of GSVs. Presumably, there might be SNARE-independent tethering mechanisms left to mediate the initial contact between GSVs and PM. However, this tethering state is usually transient and does not last long (for seconds) without the formation of SNARE complex. This finding is in agreement with a recent study by Vites and colleagues (Vites et al., 2008), who showed (using an in vitro liposome attachment assay) that the formation of *trans*-SNARE complexes on opposing membrane surfaces mediates the attachment of these surfaces. A number of studies aimed at morphometric analysis of docked vesicles at the ultrastructural level have suggested no defect in the morphologically docked vesicles from VAMP-deficient chromaffin cells (Borisovska et al., 2005).

Putting aside the problem of redundancy, the capability of capturing docked vesicles using conventional chemical fixation technique has been questioned (Rizzoli and Betz, 2004). Interestingly, recent EM analysis using high-pressure freezing has reported a significant difference in preserving labile intracellular structures as well as in localizing vesicles relative to the PM as compared with conventional fixation methods (Weimer, 2006). Another possibility is that docking in neurons is different from that of adipocytes, which is quite conceivable in view of the specialized nature of GLUT4 trafficking. Our data provide the first direct evidence that stabilized docking (for seconds) of GSVs requires the v-SNAREs.

Because the docked vesicles normally do not proceed to fusion in the absence of insulin, it is conceivable that insulin signaling might relieve certain inhibition on SNAREs and accelerate fusion through completion of *trans*-SNARE complex formation. Further studies in this direction with more focus on how SNARE complexes are regulated by insulin signaling might help to address the long-standing question in the field: where and how insulin stimulates membrane insertion of GLUT4.

## Materials and Methods

### Materials

Antibodies against VAMP2, VAMP8 and Trk (Larance et al., 2005), GLUT4 (James et al., 1988), syntaxin-4, VAMP3 (Tellam et al., 1997), VAMP7 (Wade et al., 2001), Munc18c (Widberg et al., 2003) and SNAP23 (Martin et al., 1998) have been described previously. All other antibodies were obtained as follows: mouse anti-HA antibodies from Covance Research Products (Denver, PA); Cy2, Cy3 and Cy5-conjugated secondary antibodies, from Jackson ImmunoResearch (West Grove, PA); infrared-dye-conjugated secondary antibodies from Rockland Immunochemicals (Gilbertsville, PA); rabbit 14-3-3 $\beta$  antibodies and mouse anti-GFP antibodies were obtained from Santa Cruz Biotechnology (Santa Cruz, CA). The synaptobrevin/VAMP2 heterozygous mice, on a C57Bl/6J background (Schoch et al., 2001), were from Thomas Südhof (University of Texas Southwestern, TX). The endobrevin/VAMP8 ko mice, on a mixed C57Bl/6J-129Sv background (Wang et al., 2004), were from Wanjin Hong (Institute of Molecular and Cellular Biology, Singapore).

### Plasmid construction

VAMP2 cDNAs were kindly provided by James Rothman (Columbia University, NY). The toxin-resistant (VW) mutants of VAMP3, VAMP2-GFP and VAMP3-GFP chimeras were donated by Amira Klip (University of Toronto, Canada). The cDNAs of VAMP2 and VAMP3 were amplified by polymerase chain reaction (PCR) and subcloned into *XhoI* and *BamHI* sites in the pEGFP-N1 vector (Clontech Laboratories, Palo Alto, CA). The toxin-resistant mutants of VAMP2 were cloned by PCR into the pcDNA3.1 vector (Invitrogen) with *EcoRI* and *XhoI*, and the cDNAs of VAMP7 were

cloned by PCR into the pcDNA3.1 vector with *KpnI* and *EcoRI*. The mOrange cDNA replaced eGFP in pIRES2-eGFP (Clontech Laboratories, Palo Alto, CA) using *BstXI* and *NotI*. The VAMP8 cDNA was generated by PCR and subcloned into pIRES-mOrange using *XhoI* and *EcoRI*, and also subcloned into peGFP-N1 with *XhoI* and *KpnI*. Plasmid GLUT4-eGFP was constructed as previously described (Bose et al., 2004). The monomeric Kusabira Orange (mKO) fluorescent protein cDNA replaced eGFP in peGFP-N1 using *AgeI* and *NotI*. The GLUT4 cDNA was then subcloned into pmKO-N1 with *XhoI* and *BamHI*. For the production of the GLUT4-eGFP-IRES-TeNT, firstly, the tetanus toxin (light chain) cDNA was used to substitute for eGFP in pIRES2-eGFP with *BstXI* and *NotI* and the GLUT4-eGFP cDNA was then subsequently subcloned into pIRES2-TeNT with *SmaI* and *XhoI*. The tetanus toxin (light chain) cDNA was subcloned into pIRES-mOrange with *XhoI* and *EcoRI*. The pBabe-HA-GLUT4 plasmid was as described previously (Shewan et al., 2003). The pQB125-HA-GLUT4-GFP plasmid was kindly provided by Samuel Cushman (Stanford University, Stanford, CA). The GLUT4-eGFP cDNA was subcloned into pBabe puro using *EcoRI* and *Sall*. All of the plasmids were verified by PCR sequencing.

### Transfection

Preparation and culture of adipocytes derived from MEFs was performed as described previously (Kanda et al., 2005). Seven days after commencement of differentiation, MEF-derived adipocytes were treated with 0.05% trypsin-EDTA (GIBCO) and washed twice with phosphate-buffered saline (PBS) by centrifugation at 400 *g* at room temperature. The cells were resuspended in Cytomix buffer (van den Hoff et al., 1992), and 100  $\mu$ g of GLUT4-eGFP plasmid was added to a final volume of 400  $\mu$ L. Cells were then electroporated at 200 V for 10 milliseconds using a BTX 830 electroporator (Biocompare) and plated on coverslips coated with 1% gelatin in PBS. TIRF experiments were performed 2 days after transfection in KRB solution containing (in mM) 129 NaCl, 4.7 KCl, 1.2 KH<sub>2</sub>PO<sub>4</sub>, 5 NaHCO<sub>3</sub>, 10 HEPES, 2.5 glucose, 2.5 CaCl<sub>2</sub>, 1.2 MgCl<sub>2</sub>, 0.2% BSA (pH 7.4). Prior to the imaging experiment, adipocytes were serum-starved for at least 2 hours. All TIRF experiments were performed at 30°C (Bai et al., 2007). Insulin was applied at a concentration of 100 nM throughout the study. Unless otherwise stated, all drugs were purchased from Sigma.

### TIRFM imaging collection and analysis

The TIRFM setup was constructed based on the prismless and through-the-lens configuration as previously described (Li et al., 2004). The penetration depth of the evanescent field was estimated to be 113 nm by measuring the incidence angle with a prism ( $n=1.518$ ) using a 488 nm laser beam. We randomly selected some of the green cells, which were transfected with GLUT4-eGFP-IRES-TeNT. The cells were then stimulated with 100 nM insulin, and the GLUT4-eGFP fluorescence in the evanescent field measured via TIRF. All cells measured were included in the final analysis.

### Data analysis

The method of identifying docking vesicles was described in our previous study (Bai et al., 2007). Briefly, we have developed a semi-automatic program written in Matlab (The MathWorks) for the identification of moving GSVs and detection of docking events. Fluorescence particles were automatically segmented from the background by an intensity-based threshold. Identified particles were fitted with a 2D Gaussian function to obtain the peak location and width. Because the size of GSVs should be below the diffraction limit, only particles with width of Gaussian fit smaller than 268 nm were included for further analysis. Fluorescence spots that stayed immobilized for >100 seconds probably represent clathrin-coated patches on the PM (Huang et al., 2007; our unpublished data) and were precluded from analysis. The GSVs that moved less than one pixel for more than five consecutive frames were selected for further scrutiny. The putative docked vesicles were then tracked by the 2D Gaussian-fit-based algorithm. GSVs normally docked at the PM with a dwell time ranging from one to tens of seconds, with a mean of 6.1 seconds (Bai et al., 2007).

### Purification of MEF-derived adipocyte membrane fractions and immunoblotting

Cells were washed with cold PBS, resuspended in HES buffer (20 mM HEPES, 10 mM EDTA, 250 mM sucrose pH 7.4) containing complete protease inhibitor mixture and phosphatase inhibitors (2 mM sodium orthovanadate, 1 mM pyrophosphate, 1 mM ammonium molybdate, 10 mM sodium fluoride) at 4°C and lysed by 12 passes through a 22-gauge needle followed by six passes through a 27-gauge needle. The lysate was then centrifuged at 500 *g* for 10 minutes to remove unbroken cells and at 18,000 *g* for 20 minutes to obtain the membrane fraction. All samples were subjected to SDS-PAGE analysis on 10% resolving gels. Equal amounts of protein were loaded for each sample in a single experiment. Separated proteins were electrophoretically transferred to PVDF membrane, blocked with BB (2% skim milk in 0.1% Tween 20 in PBS), and incubated with primary antibody in BB. After incubation, membranes were washed three times in BB and incubated with infrared-dye-800-conjugated secondary antibodies. Membranes were then scanned in the 800 nm channel using the Odyssey IR imager.

### HA-GLUT4 retrovirus production and infection of MEF cells

Platinum-E ecotropic packaging cells were transfected with the retrovirus vector pBabe-HA-GLUT4 (Shewan et al., 2000) using transfection reagent Lipofectamine (Invitrogen) according to the manufacturer's recommendation. Media containing recombinant retroviruses were harvested 48 hours after transfection. For infection of the target cells,  $2 \times 10^5$  MEFs were cultured in Dulbecco's modified Eagle's Medium (DMEM) containing 10% fetal bovine serum containing 4 ml of retrovirus media in 10-cm culture dishes for 24 hours, followed by selection with puromycin.

### Confocal laser scanning microscopy

MEF-derived adipocytes were cultured as described above on glass coverslips. The cells were serum-starved for 2 hours at 37°C, followed by incubation in the absence or presence of 100 nM insulin for 20 minutes. Cells were then fixed with 3% paraformaldehyde in PBS, blocked in 2% (w/v) BSA in PBS and incubated with mouse anti-HA antibodies (1:200 dilution). Cells were subsequently labeled with anti-mouse-Cy3-conjugated secondary antibodies. Optical sections were analyzed by confocal laser scanning microscopy (Leica Microsystems, Wetzlar, Germany). Image processing was carried out using Leica confocal software.

### Quantification of HA-GLUT4 PM staining

Adipocytes expressing HA-GLUT4 were incubated in the absence or presence of insulin (100 nM) for 30 minutes. Cells were labeled with HA antibody in the absence of permeabilizing agent as described previously (Larance et al., 2005). The HA-GLUT4 PM staining of adipocytes was quantified under basal and insulin-treated conditions using HCA-Vision software (<http://www.hca-vision.com/>).

### Assays of 2-deoxy-D-glucose transport

2-Deoxy-D-glucose uptake into MEF-derived adipocytes was performed as previously described for 3T3-L1 adipocytes (van Dam et al., 2005).

### LDM fractionation and staining

The low-density microsome (LDM) fraction was isolated as described previously (Larance et al., 2005) from 3T3-L1 adipocytes retrovirally infected with GLUT4-eGFP. Aliquots of 200  $\mu$ l of the collected fractions were spotted onto coverslips coated with poly-L-lysine (Sigma), bound at 4°C for 30 minutes, and then washed with cold PBS twice. The collected fractions were fixed with 3% paraformaldehyde in PBS, quenched with 50 mM glycine in PBS, and then processed for immunolabeling by permeabilization and labeling in PBS containing 0.1% saponin and 2% BSA using standard procedures. Primary antibodies were detected with Cy3- or Cy5-conjugated secondary antibodies.

### Imaging of LDM and VAMP2 wt and ko MEFs

Coverslips were examined using a Leica laser scanning confocal microscope (TCS SP2 AOBS with DM IRE2; Leica Microsystems), with a 100 $\times$  1.4 oil immersion objective and an argon laser providing 488-nm excitation lines, a HeNe laser providing 543-nm excitation lines, and a HeNe laser providing 633-nm excitation lines. The z-stacks were acquired at the optimal sampling density as defined by the Nyquist frequency. Prior to analysis, images of MEF-derived adipocytes were deconvolved using Huygens Essential Software (Scientific Volume Imaging, Hilversum, The Netherlands).

### Colocalization analysis

Colocalization was assessed in IMARIS  $\times 64$  v6.2.1 (Bitplane). The centers of mass of individual vesicles and/or structures were identified in 3D space for each channel of interest. Vesicles were considered colocalized if their centers were less than 50 nm apart.

### Statistical analysis

Data are presented as mean  $\pm$  s.e.m. and statistical analysis was performed using an unpaired Student's *t*-test. Differences at  $P < 0.05$  were considered to be statistically significant.

We thank Carsten Schmitz Peiffer, Shane Grey, Pascal Vallotton, Yan Wang, Wei Ji, Gong Peng, Dadong Wang, Changming Sun, Duncan Blair, Yvonne Ng, Masato Kasuga, Yoshikazu Tamori, Hajime Kanda, Takayuki Kawaguchi, Cynthia Corley Mastick and Will Hughes for scientific assistance. We are deeply grateful to Thomas Südhof for providing the synaptobrevin/VAMP2 knockout mice, Amira Klip for providing plasmids and Samuel Cushman for providing us with reagents. This work was supported by grants from the National Science Foundation of China (30630020), the Major State Basic Research Program of P.R. China (2004CB720000, 2006CB911002) and the Knowledge Innovation Program of the Chinese Academy of Sciences (KSCX1-YW-02-1). D.E.J. is an NHMRC Senior Principal Research Fellow and is supported by grants from the National Health and Medical Research Council of Australia.

## References

- Bai, L., Wang, Y., Fan, J., Chen, Y., Ji, W., Qu, A., Xu, P., James, D. E. and Xu, T. (2007). Dissecting multiple steps of GLUT4 trafficking and identifying the sites of insulin action. *Cell. Metab.* **5**, 47-57.
- Bajno, L., Peng, X. R., Schreiber, A. D., Moore, H. P., Trimble, W. S. and Grinstein, S. (2000). Focal exocytosis of VAMP3-containing vesicles at sites of phagosome formation. *J. Cell Biol.* **149**, 697-706.
- Bao, Y., Lopez, J. A., James, D. E. and Hunziker, W. (2008). Snapin interacts with the Exo70 subunit of the exocyst and modulates GLUT4 trafficking. *J. Biol. Chem.* **283**, 324-331.
- Borisovska, M., Zhao, Y., Tsytsyura, Y., Glyvuk, N., Takamori, S., Matti, U., Rettig, J., Sudhof, T. and Bruns, D. (2005). v-SNAREs control exocytosis of vesicles from priming to fusion. *EMBO J.* **24**, 2114-2126.
- Bose, A., Robida, S., Furciniti, P. S., Chawla, A., Fogarty, K., Corvera, S. and Czech, M. P. (2004). Unconventional myosin Myo1c promotes membrane fusion in a regulated exocytic pathway. *Mol. Cell Biol.* **24**, 5447-5458.
- Cheatham, B., Volchuk, A., Kahn, C. R., Wang, L., Rhodes, C. J. and Klip, A. (1996). Insulin-stimulated translocation of GLUT4 glucose transporters requires SNARE-complex proteins. *Proc. Natl. Acad. Sci. USA* **93**, 15169-15173.
- Chen, F., Foran, P., Shone, C. C., Foster, K. A., Melling, J. and Dolly, J. O. (1997). Botulinum neurotoxin B inhibits insulin-stimulated glucose uptake into 3T3-L1 adipocytes and cleaves cellubrevin unlike type A toxin which failed to proteolyze the SNAP-23 present. *Biochemistry* **36**, 5719-5728.
- Cosen-Binker, L. I., Binker, M. G., Wang, C. C., Hong, W. and Gaisano, H. Y. (2008). VAMP8 is the v-SNARE that mediates basolateral exocytosis in a mouse model of alcoholic pancreatitis. *J. Clin. Invest.* **118**, 2535-2551.
- Hajdúch, E., Aledo, J. C., Watts, C. and Hundal, H. S. (1997). Proteolytic cleavage of cellubrevin and vesicle-associated membrane protein (VAMP) by tetanus toxin does not impair insulin-stimulated glucose transport or GLUT4 translocation in rat adipocytes. *Biochem. J.* **321**, 233-238.
- Huang, S., Lifshitz, L. M., Jones, C., Bellve, K. D., Standley, C., Fonseca, S., Corvera, S., Fogarty, K. E. and Czech, M. P. (2007). Insulin stimulates membrane fusion and GLUT4 accumulation in clathrin coats on adipocyte plasma membranes. *Mol. Cell Biol.* **27**, 3456-3469.
- Hunt, J. M., Bommert, K., Charlton, M. P., Kistner, A., Habermann, E., Augustine, G. J. and Betz, H. (1994). A post-docking role for synaptobrevin in synaptic vesicle fusion. *Neuron* **12**, 1269-1279.
- James, D. E., Brown, R., Navarro, J. and Pilch, P. F. (1988). Insulin-regulatable tissues express a unique insulin-sensitive glucose transport protein. *Nature* **333**, 183-185.
- Jiang, L., Fan, J., Bai, L., Wang, Y., Chen, Y., Yang, L., Chen, L. and Xu, T. (2008). Direct quantification of fusion rate reveals a distal role for AS160 in insulin-stimulated fusion of GLUT4 storage vesicles. *J. Biol. Chem.* **283**, 8508-8516.
- Kanda, H., Tamori, Y., Shinoda, H., Yoshikawa, M., Sakae, M., Udagawa, J., Otani, H., Tashiro, F., Miyazaki, J. and Kasuga, M. (2005). Adipocytes from Munc18c-null mice show increased sensitivity to insulin-stimulated GLUT4 externalization. *J. Clin. Invest.* **115**, 291-301.
- Kawanishi, M., Tamori, Y., Okazawa, H., Araki, S., Shinoda, H. and Kasuga, M. (2000). Role of SNAP23 in insulin-induced translocation of GLUT4 in 3T3-L1 adipocytes. Mediation of complex formation between syntaxin4 and VAMP2. *J. Biol. Chem.* **275**, 8240-8247.
- Larance, M., Ramm, G., Stockli, J., van Dam, E. M., Winata, S., Wasinger, V., Simpson, F., Graham, M., Junutula, J. R., Guilhaus, M. et al. (2005). Characterization of the role of the Rab GTPase-activating protein AS160 in insulin-regulated GLUT4 trafficking. *J. Biol. Chem.* **280**, 37803-37813.
- Larance, M., Ramm, G. and James, D. E. (2008). The GLUT4 code. *Mol. Endocrinol.* **22**, 226-233.
- Latham, C. F., Lopez, J. A., Hu, S. H., Gee, C. L., Westbury, E., Blair, D. H., Armishaw, C. J., Alewood, P. F., Bryant, N. J., James, D. E. et al. (2006). Molecular dissection of the Munc18c/syntaxin4 interaction: implications for regulation of membrane trafficking. *Traffic* **7**, 1408-1419.
- Li, C. H., Bai, L., Li, D. D., Xia, S. and Xu, T. (2004). Dynamic tracking and mobility analysis of single GLUT4 storage vesicle in live 3T3-L1 cells. *Cell Res.* **14**, 480-486.
- Liu, Y. and Barlowe, C. (2002). Analysis of Sec22p in endoplasmic reticulum/Golgi transport reveals cellular redundancy in SNARE protein function. *Mol. Biol. Cell* **13**, 3314-3324.
- Lizunov, V. A., Matsumoto, H., Zimmerberg, J., Cushman, S. W. and Frolov, V. A. (2005). Insulin stimulates the halting, tethering, and fusion of mobile GLUT4 vesicles in rat adipose cells. *J. Cell Biol.* **169**, 481-489.
- Malsam, J., Kreye, S. and Sollner, T. H. (2008). Membrane fusion: SNAREs and regulation. *Cell Mol. Life Sci.* **65**, 2814-2832.
- Martin, L. B., Shewan, A., Millar, C. A., Gould, G. W. and James, D. E. (1998). Vesicle-associated membrane protein 2 plays a specific role in the insulin-dependent trafficking of the facilitative glucose transporter GLUT4 in 3T3-L1 adipocytes. *J. Biol. Chem.* **273**, 1444-1452.
- Ng, Y., Ramm, G., Lopez, J. A. and James, D. E. (2008). Rapid activation of Akt2 is sufficient to stimulate GLUT4 translocation in 3T3-L1 adipocytes. *Cell Metab.* **7**, 348-356.
- Olson, A. L., Knight, J. B. and Pessin, J. E. (1997). Syntaxin 4, VAMP2, and/or VAMP3/cellubrevin are functional target membrane and vesicle SNAP receptors for insulin-stimulated GLUT4 translocation in adipocytes. *Mol. Cell Biol.* **17**, 2425-2435.
- Pocard, T., Le Bivic, A., Galli, T. and Zurzolo, C. (2007). Distinct v-SNAREs regulate direct and indirect apical delivery in polarized epithelial cells. *J. Cell Sci.* **120**, 3309-3320.
- Polgar, J., Chung, S. H. and Reed, G. L. (2002). Vesicle-associated membrane protein 3 (VAMP-3) and VAMP-8 are present in human platelets and are required for granule secretion. *Blood* **100**, 1081-1083.
- Randhawa, V. K., Bilan, P. J., Khayat, Z. A., Daneman, N., Liu, Z., Ramlal, T., Volchuk, A., Peng, X. R., Coppola, T., Regazzi, R. et al. (2000). VAMP2, but not VAMP3/cellubrevin, mediates insulin-dependent incorporation of GLUT4 into the plasma membrane of L6 myoblasts. *Mol. Biol. Cell* **11**, 2403-2417.
- Rizzoli, S. O. and Betz, W. J. (2004). The structural organization of the readily releasable pool of synaptic vesicles. *Science* **303**, 2037-2039.
- Schiavo, G., Stenbeck, G., Rothman, J. E. and Sollner, T. H. (1997). Binding of the synaptic vesicle v-SNARE, synaptotagmin, to the plasma membrane t-SNARE, SNAP-25, can explain docked vesicles at neurotoxin-treated synapses. *Proc. Natl. Acad. Sci. USA* **94**, 997-1001.
- Schoch, S., Deak, F., Konigstorfer, A., Mozhayeva, M., Sara, Y., Sudhof, T. C. and Kavalali, E. T. (2001). SNARE function analyzed in synaptobrevin/VAMP knockout mice. *Science* **294**, 1117-1122.
- Shewan, A. M., Marsh, B. J., Melvin, D. R., Martin, S., Gould, G. W. and James, D. E. (2000). The cytosolic C-terminus of the glucose transporter GLUT4 contains an acidic cluster endosomal targeting motif distal to the dileucine signal. *Biochem. J.* **350**, 99-107.
- Shewan, A. M., van Dam, E. M., Martin, S., Luen, T. B., Hong, W., Bryant, N. J. and James, D. E. (2003). GLUT4 recycles via a trans-Golgi network (TGN) subdomain enriched in Syntaxins 6 and 16 but not TGN38: involvement of an acidic targeting motif. *Mol. Biol. Cell* **14**, 973-986.
- Tamori, Y., Hashimoto, M., Araki, S., Kamata, Y., Takahashi, M., Kozaki, S. and Kasuga, M. (1996). Cleavage of vesicle-associated membrane protein (VAMP)-2 and cellubrevin on GLUT4-containing vesicles inhibits the translocation of GLUT4 in 3T3-L1 adipocytes. *Biochem. Biophys. Res. Commun.* **220**, 740-745.
- Tellam, J. T., Macaulay, S. L., McIntosh, S., Hewish, D. R., Ward, C. W. and James, D. E. (1997). Characterization of Munc-18c and syntaxin-4 in 3T3-L1 adipocytes: putative role in insulin-dependent movement of GLUT-4. *J. Biol. Chem.* **272**, 6179-6186.
- Toonen, R. F., Kochubey, O., de Wit, H., Gulyas-Kovacs, A., Konijnenburg, B., Sorensen, J. B., Klingauf, J. and Verhage, M. (2006). Dissecting docking and tethering of secretory vesicles at the target membrane. *EMBO J.* **25**, 3725-3737.
- van Dam, E. M., Govers, R. and James, D. E. (2005). Akt activation is required at a late stage of insulin-induced GLUT4 translocation to the plasma membrane. *Mol. Endocrinol.* **19**, 1067-1077.
- van den Hoff, M. J., Moorman, A. F. and Lamers, W. H. (1992). Electroporation in "intracellular" buffer increases cell survival. *Nucleic Acids Res.* **20**, 2902.
- Vites, O., Florin, E. L. and Jahn, R. (2008). Docking of liposomes to planar surfaces mediated by trans-SNARE complexes. *Biophys. J.* **95**, 1295-1302.
- Voets, T., Toonen, R. F., Brian, E. C., de Wit, H., Moser, T., Rettig, J., Sudhof, T. C., Neher, E. and Verhage, M. (2001). Munc18-1 promotes large dense-core vesicle docking. *Neuron* **31**, 581-591.
- Wade, N., Bryant, N. J., Connolly, L. M., Simpson, R. J., Luzio, J. P., Piper, R. C. and James, D. E. (2001). Syntaxin 7 complexes with mouse Vps10p tail interactor 1b, syntaxin 6, vesicle-associated membrane protein (VAMP)8, and VAMP7 in b16 melanoma cells. *J. Biol. Chem.* **276**, 19820-19827.
- Wang, C. C., Ng, C. P., Lu, L., Atlashkin, V., Zhang, W., Seet, L. F. and Hong, W. (2004). A role of VAMP8/endobrevin in regulated exocytosis of pancreatic acinar cells. *Dev. Cell* **7**, 359-371.
- Wang, C. C., Shi, H., Guo, K., Ng, C. P., Li, J., Gan, B. Q., Chien Liew, H., Leinonen, J., Rajaniemi, H., Zhou, Z. H. et al. (2007). VAMP8/endobrevin as a general vesicular SNARE for regulated exocytosis of the exocrine system. *Mol. Biol. Cell* **18**, 1056-1063.
- Weimer, R. M. (2006). Preservation of *C. elegans* tissue via high-pressure freezing and freeze-substitution for ultrastructural analysis and immunocytochemistry. *Methods Mol. Biol.* **351**, 203-221.
- Widberg, C. H., Bryant, N. J., Girotti, M., Rea, S. and James, D. E. (2003). Tomosyn interacts with the t-SNAREs syntaxin4 and SNAP23 and plays a role in insulin-stimulated GLUT4 translocation. *J. Biol. Chem.* **278**, 35093-35101.
- Williams, D. and Pessin, J. E. (2008). Mapping of R-SNARE function at distinct intracellular GLUT4 trafficking steps in adipocytes. *J. Cell Biol.* **180**, 375-387.